Grain-size-dependent dielectric properties in nanograin ferroelectrics

Ziming Cai, Xiaohui Wang
State Key Laboratory of New Ceramics and Fine Processing, School of Materials Science and Engineering, Tsinghua University, Beijing 100084, PR China

Introduction: A series of ferroelectric ceramic models with grain and grain-boundary structures of different sizes are established via Voronoi tessellations. The relation between the electric displacement and electric field and the hysteresis loop are calculated using a finite element method based on a classical and modified hyperbolic tangent model via COMSOL Multiphysics.

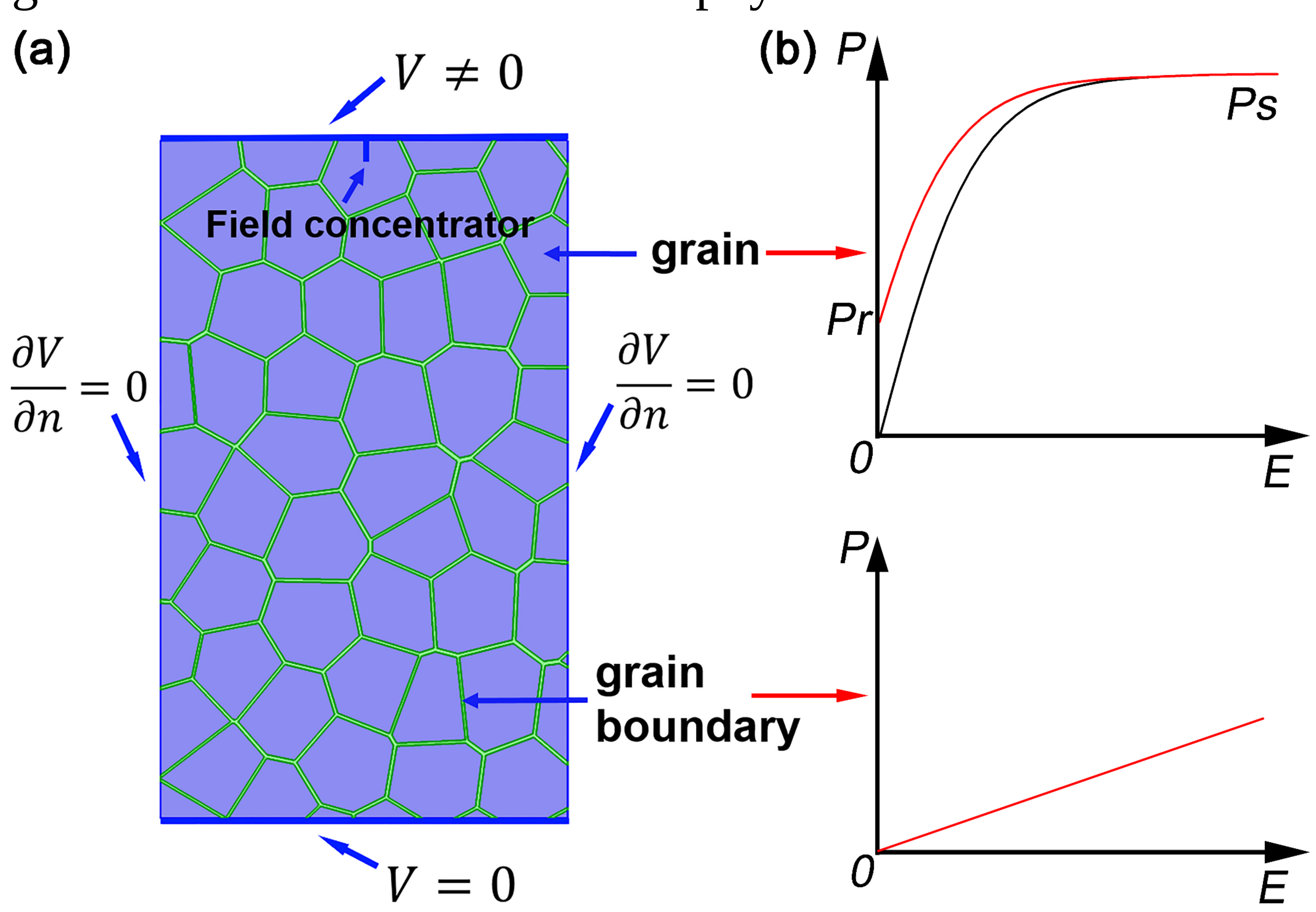

Fig. 1. Schematic of (a) the loading setup for the computational domain in phase field model and (b) the polarization response of ferroelectric ceramic grain and grain boundary. The up-branch (red curve) represents the discharging process and the down-branch (black curve) represents the charge process.

Modified hyperbolic tangent model on electric hysteresis:

1) Charge process (down branch)

$$P = P_s \tanh\left[\frac{\varepsilon_0(\varepsilon_g(0)-1)E}{P_s}\right]$$

$$\varepsilon_c' = 1 + \frac{P_s}{\varepsilon_0 E}\tanh\left[\frac{\varepsilon_0(\varepsilon_g(0)-1)E}{P_s}\right]$$

2) Discharge process (up branch)

$$P = P_s \tanh\left[\frac{\varepsilon_0(\varepsilon_g(0)-1)(E+E_c)}{P_s}\right]$$

$$\hat{\varepsilon}_c' = 1 + \frac{1}{\varepsilon_0 E}\left\{\hat{P}_s \tanh\left[\frac{\varepsilon_0(\varepsilon_g(0)-1)(E+\hat{E}_c)}{\hat{P}_s}\right] + \hat{P}_s - P_s - \hat{P}_r\right\}$$

3) Gauss' law

$$\nabla \cdot D = 0.$$

Results:

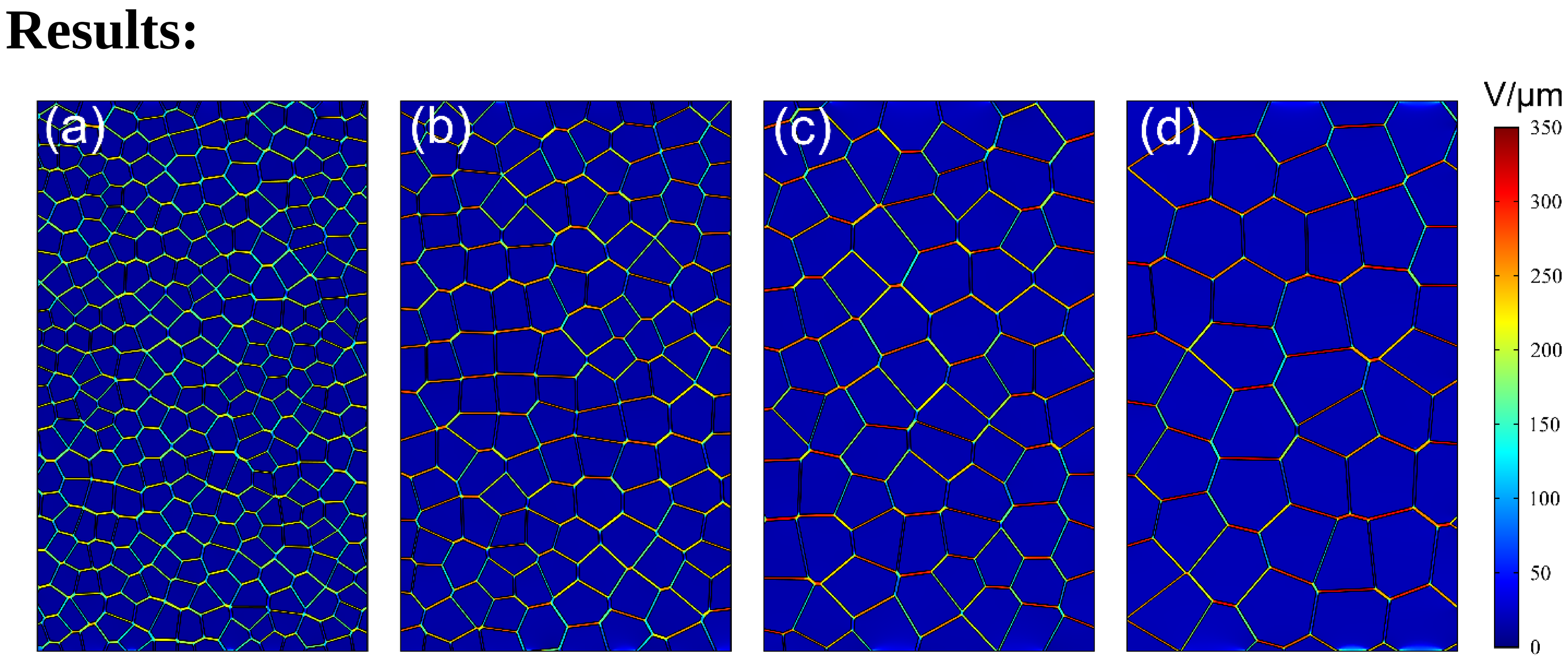

Fig. 2. Local electric field distribution of four different grain size ferroelectric ceramics: (a) 50 nm, (b) 75nm, (c) 100 nm, (d) 125 nm under the applied electric field of 30 V/μm.

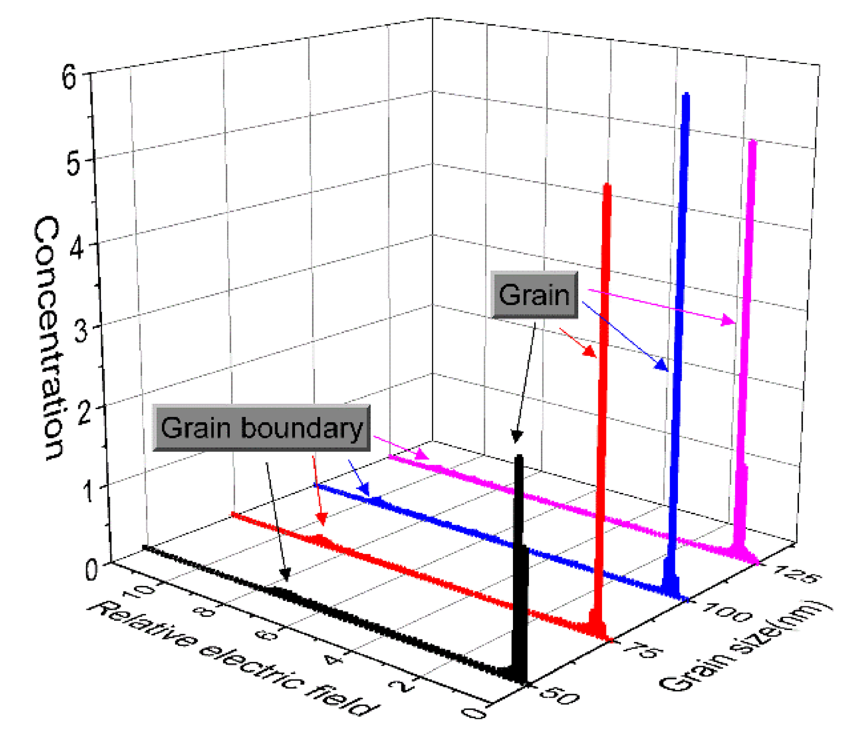

Fig. 3. Relative local electric field distribution of these ferroelectric ceramics at various grain size under a given applied electric field of 30 V/μm.

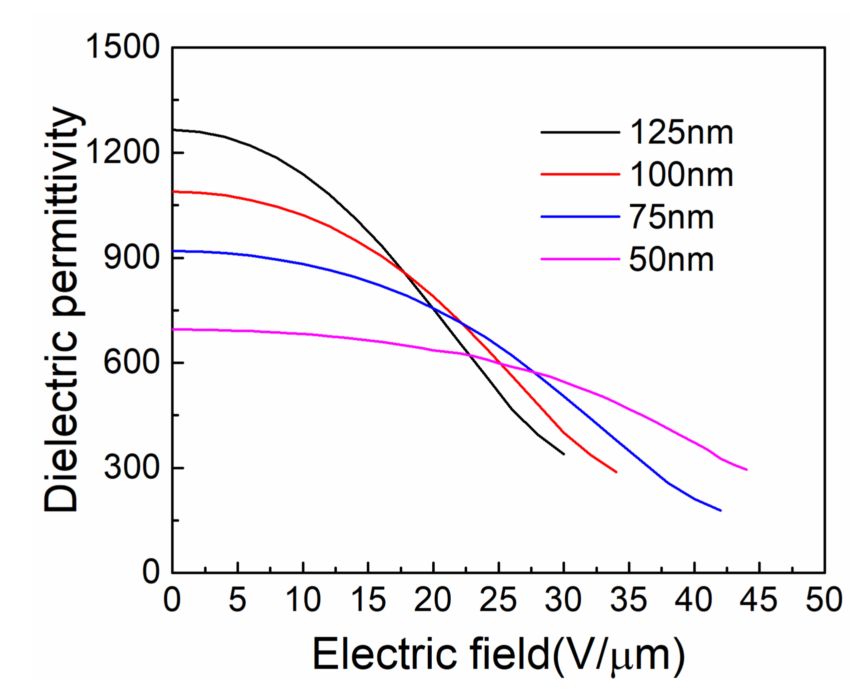

Fig. 4. Dielectric permittivity as a function of electric field of the nanostructure ferroelectric ceramics.

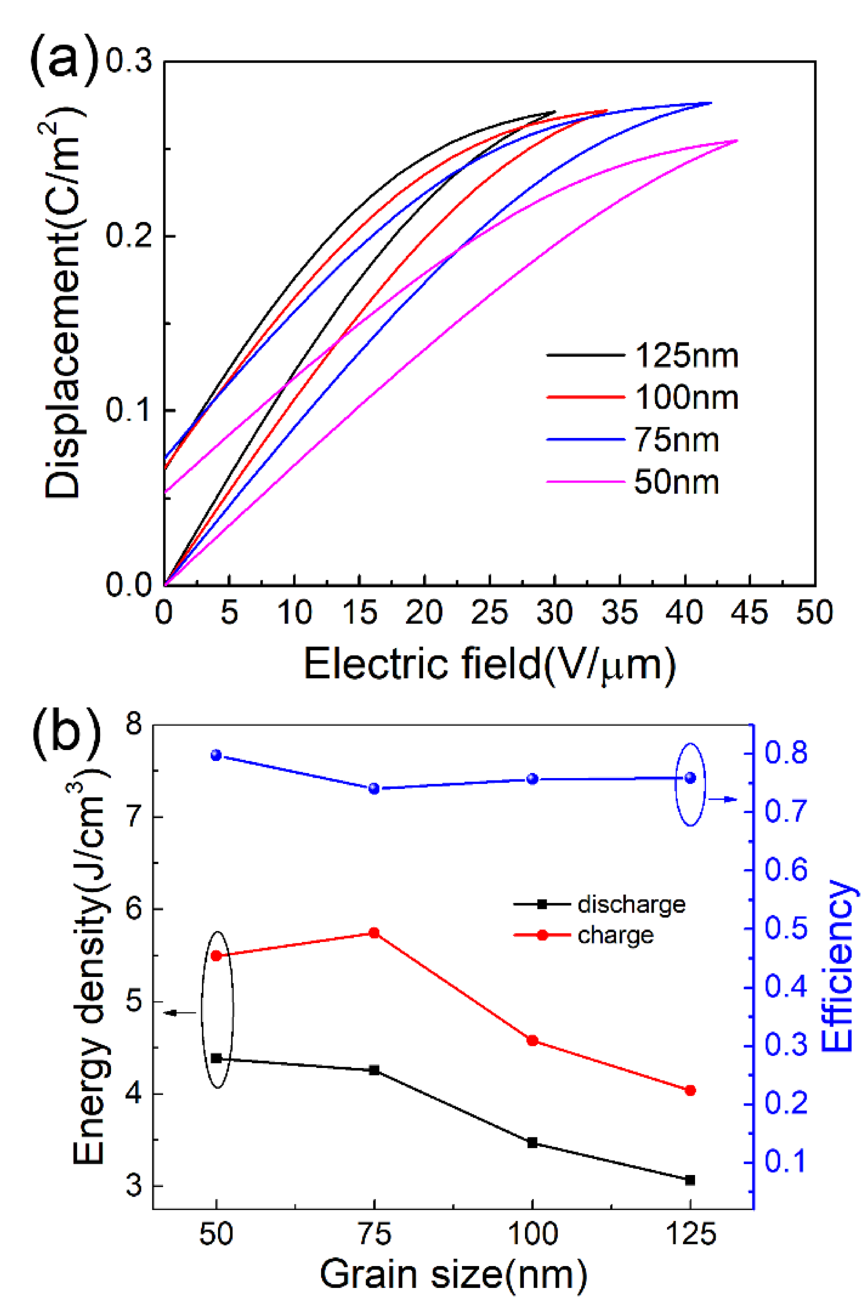

Fig. 5. (a) Electric displacement versus applied field of ferroelectric ceramics with different grain size up to their breakdown strength. (b) Energy discharge and charge density and efficiency against grain size at each breakdown point.

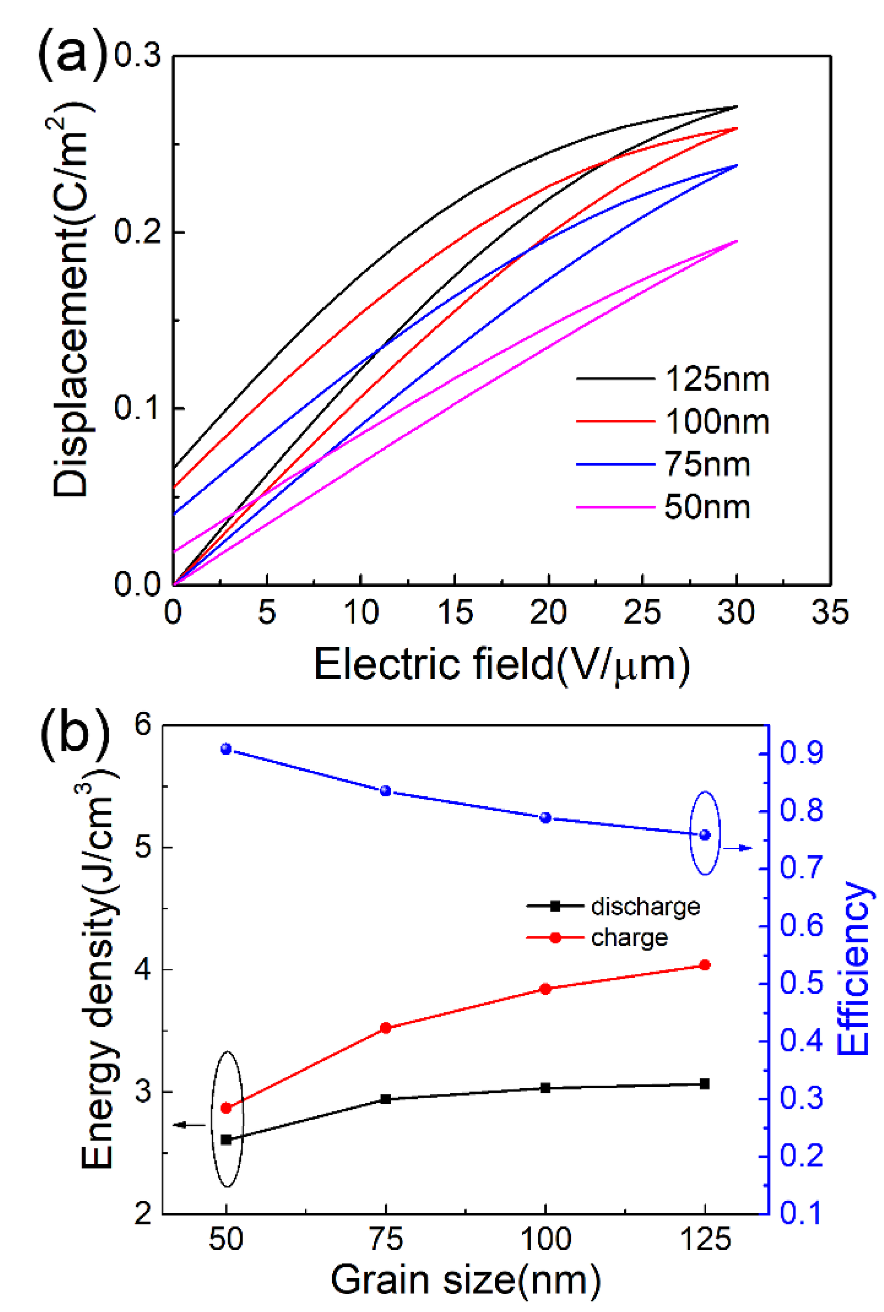

Fig. 6. (a) Electric displacement versus applied field of ferroelectric ceramics with different grain size up to 30 V/μm. (b) Energy discharge and charge density and efficiency against grain size both at the applied electric field of 30 V/μm.

Conclusion: The ferroelectric hysteresis loop are numerically calculated through a finite element method based on a classical and modified hyperbolic tangent model. It is found that as the grain size decreases, the dielectric permittivity is reduced. Under the same applied electric field, the ferroelectric ceramic with the smaller grain size possesses a lower discharge energy density but higher energy storage efficiency. When the applied electric field reaches their own breakdown strength, the smallest grain-sized ceramic displays the largest discharge energy density and energy storage efficiency. It is highly suggested that ferroelectric ceramics with smaller grain sizes can be used for applications in energy storage devices.

References:

1. Gong H, Wang X, Zhang S, et al. Grain size effect on electrical and reliability characteristics of modified fine-grained $BaTiO_3$ ceramics for mlccs. J Eur Ceram Soc. 2014;34:1733-1739.
2. Huan Y, Wang X, Fang J, et al. Grain size effects on piezoelectric properties and domain structure of $BaTiO_3$ ceramics prepared by two-step sintering. J Am Ceram Soc. 2013;96:3369-3371.
3. Zheng P, Zhang JL, Tan YQ, et al. Grain-size effects on dielectric and piezoelectric properties of poled $BaTiO_3$ ceramics. Acta Mater. 2012;60:5022-5030.